23rd Conference of the Italian Association of Aeronautics and Astronautics
AIDAA2015
Politecnico di Torino, 17-19 November 2015
E. Carrera, M. Cinefra, A. Pagani, M. Petrolo and E. Zappino (Editors)
www.aidaa2015.it

COUPLED AND UNCOUPLED THERMOELASTICITY SOLUTION FOR A ROTATING DISK USING AN ANALYTICAL METHOD

Mohammad Ali Kouchakzadeh[*], Ayoob Entezari[†], Erasmo Carrera[‡]

[*]Sharif University of Technology
Department of Aerospace Engineering
Azadi Ave, P. O. Box 11155-8639
Tehran, Iran
e-mail: mak@sharif.edu

[†]Sharif University of Technology
Department of Aerospace Engineering
Azadi Ave, P. O. Box 11155-8639
Tehran, Iran
e-mail: entezari@sharif.edu

[‡]Politecnico di Torino
Department of Mechanical and Aerospace Engineering
Corso Duca degli Abruzzi, 24
10129, Torino, Italy
e-mail: erasmo.carrera@polito.it, web page: http://www.mul2.com

Key words: Coupled thermoelasticity, Dynamic thermoelasticity, Quasi static thermoelasticity, Rotating disk, Analytical solution.

Abstarct. *In this paper, the coupled and uncoupled thermoelasticity problems for a rotating disk subjected to thermal and mechanical shock loads are analytically solved. Axisymmetric thermal and mechanical boundary conditions are considered in general forms of arbitrary heat transfer and traction, respectively, at the inner and outer radii of the disk. To solve the thermoelasticity problems based on the classical and generalized coupled theories, and dynamic and quasi static uncoupled theories, an analytical procedure based on the Fourier-Bessel transform is employed. Closed-form formulations are presented for temperature and displacement fields. The results of the present formulations are in good agreement with the numerical results available in the literature. The radial distribution and time history of temperature, displacement and stresses for the different theories of thermoelasticity in the disk are shown to provide a basis for the comparison of the results.*

1 INTRODUCTION

Rotating disks subjected to thermal loads are widely used in many engineering applications. In some of these applications, the disks may be exposed to sudden temperature changes in short periods of time. These sudden changes in temperature can cause time dependent thermal stresses in the disks. Thermal stresses due to large temperature gradients are higher than the steady state stresses. These large stresses occur before reaching the steady state condition. In such conditions, the disk should be designed with consideration of transient effects.

When a structure is exposed to a thermal shock load, the theory of uncoupled thermoelasticity does not present accurate results. In this case, the theories of coupled thermoelasticity which simulate the mutual dependency between temperature and displacement fields are necessary. In the recent years, theories of classical and generalized coupled thermoelasticity have received more attention and are developed by many researchers, due to their use in advanced structural design problems. Since the analytical solution of the coupled thermoelasticity equations are mathematically difficult to achieve, numerical methods are often used to solve these problems, especially if the boundary conditions are complicated.

Many studies have been done on the numerical methods of solution for these problems. A few number of these studies are focused on the numerical solution to the coupled thermoelasticity problem in disks. Bagri and Eslami [1] studied the generalized coupled thermoelasticity of isotropic annular disk, based on the Lord–Shulman (LS) model. They transformed the governing equations into the Laplace domain using the Laplace transform; and employed the Galerkin finite element method to solve the system of equations in the space domain. In this study, the actual physical quantities in the time domain were obtained applying the numerical inversion of the Laplace transform. Using the same method, Bakhshi et al. [2]; and Bagri and Eslami [3] based on classic and Lord–Shulman theories, respectively, studied the coupled thermoelasticity of FGM annular disk.

Number of papers that presented a closed form analytical solution for coupled thermoelasticity problems is limited. Most of the published analytical studies are limited to those of an infinite body or a half-space, where the boundary conditions are simple. In the recent years, some analytical solutions for bounded geometries with specified boundary conditions have been presented by a few researchers. The coupled thermoelasticity problem in a FGM beam are analytically solved by Abbasi et al. [4] using the finite Fourier transformation method. Afshar et al. [5] investigated two dimensional coupled thermoelasticity problem in a FGM beam subjected to lateral thermal shock. They combined the method of finite Fourier series with the Galerkin FE method to solve the govering equations. Jabbari et al. [6, 7] presented an analytical solution for the classic coupled thermoelasticity problems in spherical and cylindrical coordinates. To solve the governing equations, they used the Fourier expansion and eigenfunction methods. Following these studies and using the same methods, Jabbari and Dehbani [8, 9] obtained an analytical solution for the LS generalized coupled thermoporoelasticity problems in spherical and cylindrical coordinates. Akbarzadeh et al. [10] presented the analytical solution for coupled thermoelasticity in a FGM plate under lateral thermal shock. The analysis was based on the third-order shear deformation theory. They used the double finite Fourier series and the analytical Laplace inverse method. The coupled thermoelasticity behavior in a thick hollow cylinder based on GN model was studied by Hosseini and Abolbashari [11]. They solved the governing equations analytically using series solution in the Laplace space domain, and applied the numerical inverse Laplace transform method, to obtain displacement and temperature fields in the time domain. Shahani and Momeni [12] solved analytically the classic coupled thermoelasticity problem in a thick-walled sphere. They used the finite Hankel transform to obtain closed form solutions for temperature and displacement fields. In their study, it was assumed that temperatures and mechanical tractions on inner and outer surfaces of the sphere are specified. A fully analytical solution of the classic coupled thermoelasticity problem in a rotating disk are presented by Kouchakzadeh and Entezari [13].

The main purpose of the present study is to solve thermoelasticity problems in a rotating disk based on the classical and generalized coupled theories, and dynamic and quasi static uncoupled theories using a fully analytical procedure. The general forms of thermal and mechanical boundary conditions as arbitrary time dependent heat transfer and traction, respectively, may be prescribed at the inner and outer radii of the rotating disk. The governing equations are solved analytically using the finite Hankel transform. Finally, the analytical solutions are presented, in closed forms, for temperature and displacement fields. The results of this paper are verified by those obtained using the numerical method in Ref. [1]. The radial distributions and the time histories of temperature, displacement and stresses for the different theories of thermoelasticity in the rotating disk are shown and compared to each other.

2 GOVERNING EQUATIONS

Consider an annular rotating disk, made of isotropic material, under axisymmetric thermal and mechanical shock loads applied to its inner or outer radii. The equation of motion in radial direction for the rotating disk with constant thickness can be written as [14]

$$\frac{\partial \sigma_{rr}}{\partial r}+\frac{1}{r}\left(\sigma_{rr}-\sigma_{\theta\theta}\right)+\rho r\omega^2=\rho\frac{\partial^2 u}{\partial t^2} \tag{1}$$

where σ_{rr} and $\sigma_{\theta\theta}$ are radial and tangential stress components, r is radial coordinate, ρ is density, ω is constant angular velocity of the rotating disk, and t is the time variable. The relations between the radial displacement u and the strains are

$$\varepsilon_{rr}=\frac{\partial u}{\partial r} \quad , \quad \varepsilon_{\theta\theta}=\frac{u}{r} \tag{2}$$

where ε_{rr} and $\varepsilon_{\theta\theta}$ are the radial and tangential strain components, respectively. The stress components for the plane stress state, according to Hooke's law are

$$\begin{aligned}\sigma_{rr}&=\left(2\mu+\tilde{\lambda}\right)\varepsilon_{rr}+\tilde{\lambda}\varepsilon_{\theta\theta}-\tilde{\beta}T\\ \sigma_{\theta\theta}&=\tilde{\lambda}\varepsilon_{rr}+\left(2\mu+\tilde{\lambda}\right)\varepsilon_{\theta\theta}-\tilde{\beta}T\end{aligned} \tag{3}$$

Here, T is the temperature change and $\tilde{\lambda}$ and $\tilde{\beta}$ are obtained as

$$\tilde{\lambda} = \frac{2\mu}{\lambda + 2\mu}\lambda \quad , \quad \tilde{\beta} = \frac{2\mu}{\lambda + 2\mu}\left(3\lambda + 2\mu\right)\alpha \tag{4}$$

where λ and μ are Lame constants, and α is the coefficient of linear thermal expansion. Equations (1) to (3) may be combined to yield the equation of motion in term of the displacement component as

$$\left\{(\tilde{\lambda} + 2\mu)\left[\frac{\partial^2}{\partial r^2} + \frac{1}{r}\frac{\partial}{\partial r} - \frac{1}{r^2}\right] - \rho\frac{\partial^2}{\partial t^2}\right\}u - \tilde{\beta}\frac{\partial T}{\partial r} = -\rho r\omega^2 \tag{5}$$

For the axisymmetric problem, the classical coupled heat conduction equation in polar coordinates in the absence of heat source is obtained to be [14]

$$\left\{\kappa\left[\frac{\partial^2}{\partial r^2} + \frac{1}{r}\frac{\partial}{\partial r}\right] - \rho c\frac{\partial}{\partial t}\right\}T - \tilde{\beta}T_0\left\{\frac{\partial^2}{\partial r\partial t} + \frac{1}{r}\frac{\partial}{\partial t}\right\}u = 0 \tag{6}$$

where κ, c and T_0 are the thermal conductivity, specific heat and reference temperature, respectively.

Equations (5) and (6) constitute the governing coupled system of equations for the classical theory of thermoelasticity in the problem of isotropic rotating disk with constant thickness.

The classical coupled theory of thermoelasticity is based on the conventional energy equation (Eq. (6)). The parabolic nature of the energy equation in this theory, leads to the prediction of infinite propagation speeds for the thermal disturbances. This prediction is physically unrealistic and problems arise when we deal with special applications involving very short transient durations and sudden mechanical and thermal shock loads. On this basis, some modified coupled thermoelasticity models with the finite speed of wave propagation such as Lord-Shulman (LS), Green-Lindsay (GL), and Green–Naghdi (GN) theories have been proposed. The generalized coupled heat conduction equation based on the LS theory for the axisymmetric problem in the absence of heat source is [1, 14]

$$\begin{gathered}\left\{\kappa\left[\frac{\partial^2}{\partial r^2} + \frac{1}{r}\frac{\partial}{\partial r}\right] - \rho c\frac{\partial}{\partial t}\left(1 + t_0\frac{\partial}{\partial t}\right)\right\}T \\ -\tilde{\beta}T_0\left\{t_0\left[\frac{\partial^3}{\partial r\partial t^2} + \frac{1}{r}\frac{\partial^2}{\partial t^2}\right] + \frac{\partial^2}{\partial r\partial t} + \frac{1}{r}\frac{\partial}{\partial t}\right\}u = 0\end{gathered} \tag{7}$$

where t_0 is relaxation time associated with LS model. The relaxation time represents the time-lag needed to establish steady state heat conduction in an element of volume when a temperature gradient is suddenly imposed on the element [14, 15]. Equations (5) and (7) are the governing equations of the generalized coupled thermoelasticity based on LS model in the problem of isotropic rotating disk with constant thickness.

For the coupled equations (5) and (7), The general forms of thermal and mechanical boundary conditions can be considered as heat transfer and traction, respectively, at the inner and outer radii of the disk as follows

$$\begin{aligned} &k_{11}\left.\frac{\partial T}{\partial r}\right|_{r=r_i}+k_{12}T(r_i,t)=f_1(t) \quad , \quad k_{21}\left.\frac{\partial T}{\partial r}\right|_{r=r_o}+k_{22}T(r_o,t)=f_2(t) \\ &k_{31}\left.\frac{\partial u}{\partial r}\right|_{r=r_i}+k_{32}u(r_i,t)=f_3(t) \quad , \quad k_{41}\left.\frac{\partial u}{\partial r}\right|_{r=r_o}+k_{42}u(r_o,t)=f_4(t) \end{aligned} \tag{8}$$

where r_i and r_o are the inner and outer radii of the disk, respectively. $f_1(t)$ to $f_4(t)$ are time dependent known functions applied to the inner and outer radii. k_{ij} are constant thermal and mechanical parameters related to the conduction and convection coefficients, and mechanical properties. In general, following initial conditions may be assumed for the coupled equations (5) and (7)

$$\begin{aligned} &T(r,0)=g_1(r), \quad \dot{T}(r,0)=g_2(r) \\ &u(r,0)=g_3(r), \quad \dot{u}(r,0)=g_4(r) \end{aligned} \tag{9}$$

Here $g_1(r)$ to $g_4(r)$ are known functions of the space coordinate r. The superscript dot $(\cdot)$ denotes the differentiation with respect to time.

The governing equations may be introduced in nondimensional form for simplicity. The nondimensional parameters are defined as

$$\begin{aligned} &\hat{r}=\frac{r}{l}, && \hat{t}=\frac{tV_e}{l}, && \hat{t}_0=\frac{t_0V_e}{l} \\ &\hat{\sigma}_{rr}=\frac{\sigma_{rr}}{\tilde{\beta}T_0}, && \hat{\sigma}_{\theta\theta}=\frac{\sigma_{\theta\theta}}{\tilde{\beta}T_0}, && \hat{T}=\frac{T}{T_0} \\ &\hat{u}=\frac{(\tilde{\lambda}+2\mu)u}{l\tilde{\beta}T_0}, && \hat{\omega}=\sqrt{\frac{\rho l^2}{\tilde{\beta}T_0}}\omega \end{aligned} \tag{10}$$

where $l=k/\rho c V_e$ and $V_e=\sqrt{(\tilde{\lambda}+2\mu)/\rho}$ represent the unit length and the speed of elastic wave propagation, respectively [1, 14]. The hat values indicate nondimensional parameters. Using the nondimensional parameters, the governing coupled system of Eqs. (5) and (7), and stress-displacement relations take the form

$$\begin{aligned} &\left\{\frac{\partial^2}{\partial\hat{r}^2}+\frac{1}{\hat{r}}\frac{\partial}{\partial\hat{r}}-\frac{\partial}{\partial\hat{t}}\left(1+\hat{t}_0\frac{\partial}{\partial\hat{t}}\right)\right\}\hat{T} \\ &-C\left\{\hat{t}_0\left[\frac{\partial^3}{\partial\hat{r}\partial\hat{t}^2}+\frac{1}{\hat{r}}\frac{\partial^2}{\partial\hat{t}^2}\right]+\frac{\partial^2}{\partial\hat{r}\partial\hat{t}}+\frac{1}{\hat{r}}\frac{\partial}{\partial\hat{t}}\right\}\hat{u}=0 \end{aligned} \tag{11}$$

$$\left\{\frac{\partial^2}{\partial \hat{r}^2}+\frac{1}{\hat{r}}\frac{\partial}{\partial \hat{r}}-\frac{1}{\hat{r}^2}-\frac{\partial^2}{\partial \hat{t}^2}\right\}\hat{u}-\frac{\partial \hat{T}}{\partial \hat{r}}=-\hat{r}\hat{\omega}^2 \tag{12}$$

$$\begin{aligned}\hat{\sigma}_{rr}&=\frac{\partial \hat{u}}{\partial \hat{r}}+\frac{\tilde{\lambda}}{(\tilde{\lambda}+2\mu)}\frac{\hat{u}}{\hat{r}}-\hat{T}\\ \hat{\sigma}_{\theta\theta}&=\frac{\tilde{\lambda}}{(\tilde{\lambda}+2\mu)}\frac{\partial \hat{u}}{\partial \hat{r}}+\frac{\hat{u}}{\hat{r}}-\hat{T}\end{aligned} \tag{13}$$

where $C = T_0\tilde{\beta}^2 \big/ \rho c(\tilde{\lambda}+2\mu)$ is called the thermoelastic coupling (or damping) parameter [14]. For a certain isotropic material, the thermoelastic coupling parameter is a function of the reference temperature T_0.

From nondimensional Eqs. (11) and (12), the thermal disturbances propagate with the speed of $V_t = \sqrt{1/\hat{t}_0}$ and the speed of propagation of the elastic disturbances is unity [14, 16]. The value of V_t is finite for the Lord–Shulman theory. When the relaxation time is zero, the system of Eqs. (11) and (12) reduces to that of the classical coupled thermoelasticity which predicts an infinite speed of propagation of thermal disturbances.

The boundary and initial conditions (8) and (9) in terms of the nondimensional parameters can be written in the form

$$\begin{aligned}&\hat{k}_{11}\left.\frac{\partial \hat{T}}{\partial \hat{r}}\right|_{\hat{r}=a}+\hat{k}_{12}\hat{T}(a,t)=\hat{f}_1(\hat{t})\\ &\hat{k}_{21}\left.\frac{\partial \hat{T}}{\partial \hat{r}}\right|_{\hat{r}=b}+\hat{k}_{22}\hat{T}(b,t)=\hat{f}_2(\hat{t})\\ &\hat{k}_{31}\left.\frac{\partial \hat{u}}{\partial \hat{r}}\right|_{\hat{r}=a}+\hat{k}_{32}\hat{u}(a,t)=\hat{f}_3(\hat{t})\\ &\hat{k}_{41}\left.\frac{\partial \hat{u}}{\partial \hat{r}}\right|_{\hat{r}=b}+\hat{k}_{42}\hat{u}(b,t)=\hat{f}_4(\hat{t})\\ &\hat{T}(\hat{r},0)=\hat{g}_1(\hat{r}),\quad \dot{\hat{T}}(\hat{r},0)=\hat{g}_2(\hat{r})\\ &\hat{u}(\hat{r},0)=\hat{g}_3(\hat{r}),\quad \dot{\hat{u}}(\hat{r},0)=\hat{g}_4(\hat{r})\end{aligned} \tag{14}$$

Here a and b are the nondimensional inner and outer radii, respectively. The hat values are nondimensional parameters that are defined as

$$\begin{aligned}
&\hat{k}_{11}=\frac{k_{11}}{\kappa}, && \hat{k}_{12}=\frac{k_{12}l}{\kappa}, && \hat{f}_1(\hat{t})=\frac{lf_1(t)}{\kappa T_0}\\
&\hat{k}_{21}=\frac{k_{21}}{\kappa}, && \hat{k}_{22}=\frac{k_{22}l}{\kappa}, && \hat{f}_2(\hat{t})=\frac{lf_2(t)}{\kappa T_0}\\
&\hat{k}_{31}=\frac{k_{31}}{(\tilde{\lambda}+2\mu)}, && \hat{k}_{32}=\frac{k_{32}l}{(\tilde{\lambda}+2\mu)}, && \hat{f}_3(\hat{t})=\frac{f_3(t)}{\tilde{\beta}T_0}\\
&\hat{k}_{41}=\frac{k_{41}}{(\tilde{\lambda}+2\mu)}, && \hat{k}_{42}=\frac{k_{42}l}{(\tilde{\lambda}+2\mu)}, && \hat{f}_4(\hat{t})=\frac{f_4(t)}{\tilde{\beta}T_0}\\
&\hat{g}_1(\hat{r})=\frac{g_1(r)}{T_0}, && \hat{g}_2(\hat{r})=\frac{lg_2(r)}{T_0V_e}\\
&\hat{g}_3(\hat{r})=\frac{(\tilde{\lambda}+2\mu)g_3(r)}{l\tilde{\beta}T_0}, && \hat{g}_4(\hat{r})=\frac{(\tilde{\lambda}+2\mu)g_4(r)}{\tilde{\beta}T_0V_e}
\end{aligned} \tag{15}$$

As is evident from Eqs. (11) and (12), The theories of coupled thermoelasticity take into account the time rate of change of the first invariant of strain tensor in the first law of thermodynamics causing the coupling between elasticity and energy equations. This situation occurs when the rate of application of a thermo-mechanical load is rapid enough to produce thermal stress waves [14]. To obtain the solution for temperature and displacements and finally the stresses, these coupled equations must be solved simultaneously.

If the time rate of change of imposed thermo-mechanical loads is not large enough to excite the thermal stress wave propagation, the effect of coupling term in the energy equation (11) can be negligible. In this case, the energy equation of the classical coupled theory reduces to

$$\left\{\frac{\partial^2}{\partial\hat{r}^2}+\frac{1}{\hat{r}}\frac{\partial}{\partial\hat{r}}-\frac{\partial}{\partial\hat{t}}\right\}\hat{T}=0 \tag{16}$$

Equations (12) and (16) are the governing equations of the dynamic uncoupled thermaoelasticity for the rotating disk.

In most practical engineering problems the imposed thermo-mechanical load is vary sufficiently slowly with the time so as not to excite inertia effects. Such problems are called quasi-static [14]. Neglecting the inertia term, the equation of motion (12) reduces to

$$\left\{\frac{\partial^2}{\partial\hat{r}^2}+\frac{1}{\hat{r}}\frac{\partial}{\partial\hat{r}}-\frac{1}{\hat{r}^2}\right\}\hat{u}-\frac{\partial\hat{T}}{\partial\hat{r}}=-\hat{r}\hat{\omega}^2 \tag{17}$$

Therefore, the quasi-static uncoupled thermoelasticity problem in the rotating disk can be described by Eqs. (16) and (17). For a steady-state condition the heat conduction Eq. (16) is further reduced to [14]

$$\left\{\frac{\partial^2}{\partial \hat{r}^2}+\frac{1}{\hat{r}}\frac{\partial}{\partial \hat{r}}\right\}\hat{T}=0 \tag{18}$$

This equation along with the imposed boundary conditions fully defines the field of temperature distribution in the disk for the steady state.

3 SOLUTION OF CUOPLED THERMOELASTICITY

The governing Equations (11) and (12) are a system of second order linear partial differential equations (PDE) with nonconstant (radius dependent) coefficients subjected to the nonhomogeneous initial and boundary conditions. These equations can be solved using the analytical method based on the finite Hankel transform, which can change the partial differential equations into solvable ordinary differential equations. To this end, first, the principle of superposition can be used to simplify the coupled initial-boundary value problem (IBVP) into simpler sub-IBVPs.

Therefore, using the principle of superposition, the heat conduction Equation (11) along with the corresponding boundary and initial conditions (14) in terms of the nondimensional parameters (without the hat sign for convenience), can be decomposed into two following sub-IBVPs

$$\begin{aligned}
&\frac{\partial^2 T_1}{\partial r^2}+\frac{1}{r}\frac{\partial T_1}{\partial r}-\dot{T}_1-t_0\ddot{T}_1=0\\
&k_{11}\left.\frac{\partial T_1}{\partial r}\right|_{r=a}+k_{12}T_1(a,t)=f_1(t) \quad , \quad k_{21}\left.\frac{\partial T_1}{\partial r}\right|_{r=b}+k_{22}T_1(b,t)=f_2(t)\\
&T_1(r,0)=0 \quad , \quad \dot{T}_1(r,0)=0
\end{aligned} \tag{19}$$

$$\begin{aligned}
&\frac{\partial^2 T_2}{\partial r^2}+\frac{1}{r}\frac{\partial T_2}{\partial r}-\dot{T}_2-t_0\ddot{T}_2=C\left\{t_0\left(\ddot{u}_{,r}+\frac{\ddot{u}}{r}\right)+\dot{u}_{,r}+\frac{\dot{u}}{r}\right\}\\
&k_{11}\left.\frac{\partial T_2}{\partial r}\right|_{r=a}+k_{12}T_2(a,t)=0 \quad , \quad k_{21}\left.\frac{\partial T_2}{\partial r}\right|_{r=b}+k_{22}T_2(b,t)=0\\
&T_2(r,0)=g_1(r) \quad , \quad \dot{T}_2(r,0)=g_2(r)
\end{aligned} \tag{20}$$

Note that in the first sub problem, the PDE is homogeneous while the boundary and initial conditions are nonhomogeneous and homogeneous, respectively. In the second sub problem, the PDE is nonhomogeneous and may include the coupled terms while the boundary and initial conditions are homogeneous and nonhomogeneous, respectively. Similarly, Eqs. (12) and (14) may be decomposed into two following sub-IBVPs

$$\begin{aligned}
&\frac{\partial^2 u_1}{\partial r^2}+\frac{1}{r}\frac{\partial u_1}{\partial r}-\frac{u_1}{r^2}-\ddot{u}_1=0\\
&k_{31}\left.\frac{\partial u_1}{\partial r}\right|_{r=a}+k_{32}u_1(a,t)=f_3(t)\quad,\quad k_{41}\left.\frac{\partial u_1}{\partial r}\right|_{r=b}+k_{42}u_1(b,t)=f_4(t)\\
&u_1(r,0)=0\quad,\quad \dot{u}_1(r,0)=0
\end{aligned}\tag{21}$$

$$\begin{aligned}
&\frac{\partial^2 u_2}{\partial r^2}+\frac{1}{r}\frac{\partial u_2}{\partial r}-\frac{u_2}{r^2}-\ddot{u}_2=T_{,r}-r\omega^2\\
&k_{31}\left.\frac{\partial u_2}{\partial r}\right|_{r=a}+k_{32}u_2(a,t)=0\quad,\quad k_{41}\left.\frac{\partial u_2}{\partial \hat{r}}\right|_{r=b}+k_{42}u_2(b,t)=0\\
&u_2(r,0)=g_3(r)\ ,\ \dot{u}_2(r,0)=g_4(r)
\end{aligned}\tag{22}$$

The final solution for the temperature and displacement fields is obtained from total of two solutions of these sub-IBVPs as follows

$$T(r,t)=T_1(r,t)+T_2(r,t)\quad,\quad u(r,t)=u_1(r,t)+u_2(r,t)\tag{23}$$

where, The solutions of homogeneous equation corresponding to heat conduction and motion equations are shown by $T_1(r,t)$ and $u_1(r,t)$, respectively. $T_2(r,t)$ and $u_2(r,t)$ are solutions of nonhomogeneous form of heat conduction and motion equations, respectively.
Equations (19) and (21) are called Bessel equations and can be separately solved using finite Hankel transform. Using the definition of the finite Hankel transform, the transformed temperature and displacement can expressed as

$$\begin{aligned}
\mathcal{H}[T_1(r,t)]&=\bar{T}_1(t,\xi_m)=\int_a^b rT_1(r,t)K_0(r,\xi_m)dr\\
\mathcal{H}[u_1(r,t)]&=\bar{u}_1(t,\eta_n)=\int_a^b ru_1(r,t)K_1(r,\eta_n)dr
\end{aligned}\tag{24}$$

Here $K_0(r,\xi_m)$ and $K_1(r,\eta_n)$ are the kernel functions related to Eqs. (19) and (21), respectively, and result in the following relations [17]

$$\begin{aligned}
K_0(r,\xi_m)=\ &J_0(\xi_m r)\left(k_{21}\left.\frac{\partial Y_0(\xi_m r)}{\partial r}\right|_{r=b}+k_{22}Y_0(\xi_m b)\right)\\
&-Y_0(\xi_m r)\left(k_{21}\left.\frac{\partial J_0(\xi_m r)}{\partial r}\right|_{r=b}+k_{22}J_0(\xi_m b)\right)
\end{aligned}\tag{25}$$

$$K_1(r,\eta_n) = J_1(\eta_n r)\left(k_{41}\left.\frac{\partial Y_1(\eta_n r)}{\partial r}\right|_{r=b} + k_{42}Y_1(\eta_n b)\right) - Y_1(\eta_n r)\left(k_{41}\left.\frac{\partial J_1(\eta_n r)}{\partial r}\right|_{r=b} + k_{42}J_1(\eta_n b)\right) \quad (26)$$

where $J_\nu(\xi_m r)$ and $Y_\nu(\xi_m r)$ (or $J_\nu(\eta_n r)$ and $Y_\nu(\eta_n r)$) are the Bessel functions of the first and second kind, and of order $\nu, (\nu = 0\ and\ 1)$. ξ_m and η_n are positive roots of the following equations, respectively [17]

$$\left(k_{11}\left.\frac{\partial Y_0(\xi_m r)}{\partial r}\right|_{r=a} + k_{12}Y_0(\xi_m a)\right)\left(k_{21}\left.\frac{\partial J_0(\xi_m r)}{\partial r}\right|_{r=b} + k_{22}J_0(\xi_m b)\right) - \left(k_{21}\left.\frac{\partial Y_0(\xi_m r)}{\partial r}\right|_{r=b} + k_{22}Y_0(\xi_m b)\right)\left(k_{11}\left.\frac{\partial J_0(\xi_m r)}{\partial r}\right|_{r=a} + k_{12}J_0(\xi_m a)\right) = 0 \quad (27)$$

$$\left(k_{31}\left.\frac{\partial Y_1(\eta_n r)}{\partial r}\right|_{r=a} + k_{32}Y_1(\eta_n a)\right)\left(k_{41}\left.\frac{\partial J_1(\eta_n r)}{\partial r}\right|_{r=b} + k_{42}J_1(\eta_n b)\right) - \left(k_{41}\left.\frac{\partial Y_1(\eta_n r)}{\partial r}\right|_{r=b} + k_{42}Y_1(\eta_n b)\right)\left(k_{31}\left.\frac{\partial J_1(\eta_n r)}{\partial r}\right|_{r=a} + k_{32}J_1(\eta_n a)\right) = 0 \quad (28)$$

Equations (27) and (28) have an infinite number of the roots, because the Bessel functions are periodic. According to the properties of Sturm-Liouville problem, the kernel functions are orthogonal with respect to the weight function r. Taking the finite Hankel transform of Eqs. (19) and (21), and then using the operational properties on the derivatives [17], leads to

$$t_0\ddot{\bar{T}}_1 + \dot{\bar{T}}_1 + \xi_m^2\bar{T}_1 = A_1(t) \quad (29)$$

$$\ddot{\bar{u}}_1 + \eta_n^2\bar{u}_1 = A_2(t) \quad (30)$$

where

$$A_1(t) = \frac{2}{\pi}\left(f_2(t) - \frac{d_2}{d_1}f_1(t)\right) \quad (31)$$

$$A_2(t) = \frac{2}{\pi}\left(f_4(t) - \frac{d_4}{d_3}f_3(t)\right) \quad (32)$$

and

$$\begin{aligned} d_1 &= k_{11} \left.\frac{\partial J_0(\xi_m r)}{\partial r}\right|_{r=a} + k_{12} J_0(\xi_m a) \quad , \quad d_2 = k_{21} \left.\frac{\partial J_0(\xi_m r)}{\partial r}\right|_{r=b} + k_{22} J_0(\xi_m b) \\ d_3 &= k_{31} \left.\frac{\partial J_1(\eta_n r)}{\partial r}\right|_{r=a} + k_{32} J_1(\eta_n a) \quad , \quad d_4 = k_{41} \left.\frac{\partial J_1(\eta_n r)}{\partial r}\right|_{r=b} + k_{42} J_1(\eta_n b) \end{aligned} \tag{33}$$

$\bar{T}_1$ and $\bar{u}_1$ are obtained by solving the nonhomogeneous second order differential equations (29) and (30), respectively, as follows

$$\bar{T}_1(t) = \frac{1}{\Delta} \int_0^t A_1(\tau) \left[e^{\frac{1}{2t_0}\tau + \frac{\Delta}{2t_0}(2t-\tau)} - e^{\frac{1+\Delta}{2t_0}(\tau - t)} \right] d\tau \tag{34}$$

$$\bar{u}_1(t, \eta_n) = \frac{1}{\eta_n} \int_0^t A_2(\tau) \sin\big(\eta_n (t-\tau)\big) d\tau \tag{35}$$

where $\Delta = \sqrt{1 - 4t_0\xi_m^2}$. The inverse finite Hankel transforms of Eqs. (24) can be defined by the following series [17]

$$\begin{aligned} \mathcal{H}^{-1}[\bar{T}_1(t,\xi_m)] &= T_1(r,t) = \sum_{m=1}^{\infty} \tilde{a}_m \bar{T}_1(t,\xi_m) K_0(r,\xi_m) \\ \mathcal{H}^{-1}[\bar{u}_1(t,\eta_n)] &= u_1(r,t) = \sum_{n=1}^{\infty} \tilde{b}_n \bar{u}_1(t,\eta_n) K_1(r,\eta_n) \end{aligned} \tag{36}$$

where the coefficients of the series can be computed as

$$\tilde{a}_m = 1 \Big/ \left\| K_0(r,\xi_m) \right\|^2 \qquad , \qquad \tilde{b}_n = 1 \Big/ \left\| K_1(r,\eta_n) \right\|^2 \tag{37}$$

$\left\| K_0(r,\xi_m) \right\|^2$ and $\left\| K_1(r,\eta_n) \right\|^2$ are the square of the norm of $K_0(r,\xi_m)$ and $K_1(r,\eta_n)$, respectively, on the interval $[a,b]$ with weight function r, and are defined as

$$\left\| K_0(r,\xi_m) \right\|^2 = \int_a^b r \left[K_0(r,\xi_m) \right]^2 dr \qquad , \qquad \left\| K_1(r,\eta_n) \right\|^2 = \int_a^b r \left[K_1(r,\eta_n) \right]^2 dr \tag{38}$$

Due to the orthogonality properties of the kernel functions, the solutions of Eqs. (20) and (22), $T_2(r,t)$ and $u_2(r,t)$, can be expanded in terms of functions $K_0(r,\xi_m)$ and $K_1(r,\eta_n)$, respectively as follows

$$T_2(r,t) = \sum_{m=1}^{\infty} \sum_{n=1}^{\infty} Q_{mn}(t) K_0(r,\xi_m) \quad , \quad u_2(r,t) = \sum_{m=1}^{\infty} \sum_{n=1}^{\infty} S_{mn}(t) K_1(r,\eta_n) \tag{39}$$

where $Q_{mn}(t)$ and $S_{mn}(t)$ are unknown time dependent functions to be found. Substituting Eqs. (36) and (39) into Eqs. (20) and (22) and simplifying yields

$$\begin{aligned}&\left(t_0\ddot{Q}_{mn}+\dot{Q}_{mn}+\xi_m^2 Q_{mn}\right)K_0(r,\xi_m)\\&=-C\left\{t_0\ddot{S}_{mn}+\dot{S}_{mn}+t_0\tilde{b}_n\ddot{\bar{u}}_1+\tilde{b}_n\dot{\bar{u}}_1\right\}\left(\frac{\partial K_1(r,\eta_n)}{\partial r}+\frac{K_1(r,\eta_n)}{r}\right)\end{aligned} \tag{40}$$

$$\left(\ddot{S}_{mn}+\eta_n^2 S_{mn}\right)K_1(r,\eta_n)=r\omega^2-\frac{\partial K_0(r,\xi_m)}{\partial r}\left(Q_{mn}+\tilde{a}_m\bar{T}_1\right) \tag{41}$$

Using the orthogonality conditions for $K_0(r,\xi_m)$ and $K_1(r,\eta_n)$, multiplying both sides of Eqs. (40) and (41) by $rK_0(r,\xi_k)$ and $rK_1(r,\eta_j)$, respectively, and integrating from a to b, yields

$$t_0\ddot{Q}_{mn}+\dot{Q}_{mn}+\xi_m^2 Q_{mn}=CU_1\left\{t_0\ddot{S}_{mn}+\dot{S}_{mn}+t_0\tilde{b}_n\ddot{\bar{u}}_1+\tilde{b}_n\dot{\bar{u}}_1\right\} \tag{42}$$

$$\ddot{S}_{mn}+\eta_n^2 S_{mn}=U_2\left(Q_{mn}+\tilde{a}_m\bar{T}_1\right)+U_3\omega^2 \tag{43}$$

where

$$\begin{aligned}&U_1=-\frac{\int_a^b rK_0(r,\xi_m)\left\{\frac{\partial K_1(r,\eta_n)}{\partial r}+\frac{K_1(r,\eta_n)}{r}\right\}dr}{\left\|K_0(r,\xi_m)\right\|^2}\\&U_2=-\frac{\int_a^b rK_1(r,\eta_n)\frac{\partial K_0(r,\xi_m)}{\partial r}dr}{\left\|K_1(r,\eta_n)\right\|^2}\quad,\quad U_3=\frac{\int_a^b r^2K_1(r,\eta_n)dr}{\left\|K_1(r,\eta_n)\right\|^2}\end{aligned} \tag{44}$$

Also, according to the the orthogonality conditions, by substituting Eqs. (39) into (20) and (22), respectively, the initial conditions for Eqs. (42) and (43) can be obtained.
To solve the coupled Eqs. (42) and (43), they are decoupled by eliminating Q_{mn} from Eq. (42) using Eq. (43). Upon elimination, the decoupled equation is written as

$$\begin{aligned}&t_0S^{(4)}{}_{mn}+\dddot{S}_{mn}+\left(\xi_m^2+t_0\eta_n^2-Ct_0U_1U_2\right)\ddot{S}_{mn}+\left(\eta_n^2-CU_1U_2\right)\dot{S}_{mn}+\xi_m^2\eta_n^2S_{mn}\\&=CU_1U_2\tilde{b}_n\left(t_0\dddot{\bar{u}}_1+\ddot{\bar{u}}_1\right)+U_2\tilde{a}_m\left(t_0\ddot{\bar{T}}_1+\dot{\bar{T}}_1+\xi_m^2\bar{T}_1\right)+\xi_m^2\omega^2U_3\end{aligned} \tag{45}$$

Substituting Eqs. (29) into Eq. (45) yields

$$\begin{aligned} & t_0 S^{(4)}{}_{mn} + \dddot{S}_{mn} + \left(\xi_m^2 + t_0\eta_n^2 - Ct_0U_1U_2\right)\ddot{S}_{mn} + \left(\eta_n^2 - CU_1U_2\right)\dot{S}_{mn} + \xi_m^2\eta_n^2 S_{mn} \\ & = CU_1U_2\tilde{b}_n\left(t_0\dddot{\bar{u}}_1 + \dot{\bar{u}}_1\right) + U_2\tilde{a}_m A_1(t) + \xi_m^2\omega^2 U_3 \end{aligned} \tag{46}$$

$Q_{mn}(t)$ can be obtained by solving Eq. (46) for $S_{mn}(t)$ and substituting into Eq. (43) as

$$Q_{mn}(t) = \frac{1}{U_2}\left(\ddot{S}_{mn} + \eta_n^2 S_{mn} - \omega^2 U_3\right) - \tilde{a}_m \bar{T}_1 \tag{47}$$

Euation (46) is a nonhomogeneous ordinary differential equation with constant coefficients and has general and particular solutions. The complete solution of this equation may be represented as

$$S_{mn}(t) = S^g_{mn}(t) + S^p_{mn}(t) \tag{48}$$

where $S^g_{mn}(t)$ is a general solution of Eq. (46), with the right-hand terms equal zero. $S^p_{mn}(t)$ is particular solutions which is related to boundary conditions of the problem and angular velocity of the disk. The characteristic polynomial corresponding to Eq. (46) is

$$t_0 s^4 + s^3 + \left(\xi_m^2 + t_0\eta_n^2 - CU_1U_2t_0\right)s^2 + \left(\eta_n^2 - CU_1U_2\right)s + \xi_m^2\eta_n^2 = 0 \tag{49}$$

Solving Eq. (49) for every value of m and n gives four pairs of complex conjugate roots $s_{mn,i}(i = 1,\ldots,4)$, with a negative real part and an imaginary part. These roots cause four modes of mechanichal oscillation related to the function $S_{mn}(t)$. The period and frequency of the oscillation only depend on the imaginary part. The damping of this oscillation is caused by the negative real part, which means the thermomechanical oscillation is stable.
Thus, the general solution of Eq. (46) with the right-hand terms equal zero is obtained as

$$S^g_{mn}(t) = \sum_{i=1}^{4} c_i e^{s_{mn,i}t} \tag{50}$$

where the constant coefficients c_i are determined by substituting the complete solution of Eq. (46) into the initial conditions.
Finally, the closed form solutions for the nondimensional temperature and displacement fields obtained from solving the governing coupled system of Eqs. (11) and (12), can be stated as follows

$$\begin{aligned} T(r,t) &= \sum_{m=1}^{\infty}\tilde{a}_m\bar{T}_1(t,\xi_m)K_0(r,\xi_m) + \sum_{m=1}^{\infty}\sum_{n=1}^{\infty}Q_{mn}(t)K_0(r,\xi_m) \\ u(r,t) &= \sum_{n=1}^{\infty}\tilde{b}_n\bar{u}_1(t,\eta_n)K_1(r,\eta_n) + \sum_{m=1}^{\infty}\sum_{n=1}^{\infty}S_{mn}(t)K_1(r,\eta_n) \end{aligned} \tag{51}$$

The expressions for the stress components in the disk are determined by substituting Eqs. (51) into (13). When the relaxation time is zero ($\hat{t}_0 = 0$), the same mathematical procedure may be used to solve the classical coupled thermoelastic equations.

4 SOLUTION OF UNCUOPLED THERMOELASTICITY

In the case of dynamic uncoupled thermaoelasticity problem in the rotating disk ($C = 0$ and the effect of inertia term is considered), the solutions to uncoupled equations (12) and (16) can be separately obtained using the finite Hankel transform in a similar manner to that of coupled problems.

For the case of the quasi-static thermoelasticity problem, the differential equation of heat conduction (16) is a Bessel-type equation. This equation can be solved in a similar way to the previous problems to yield the temperature field. The equation of motion (17) can be written in the following form

$$\frac{\partial}{\partial r}\left[\frac{1}{r}\frac{\partial}{\partial r}(ru)\right] = \frac{\partial T}{\partial r} - r\omega^2 \tag{52}$$

Integrating Eq. (52) twice and designating the two integration constants as $c_1(t)$ and $c_2(t)$ gives the radial displacement as

$$u(r,t) = \frac{1}{r}\int_a^r T(r,t)rdr - \frac{1}{8}r^3\omega^2 + rc_1(t) + \frac{c_2(t)}{r} \tag{53}$$

By substituting Eq. (53) into Eqs. (13), without the hat sign for convenience, the stress components are obtained as

$$\begin{aligned}\sigma_{rr} = &-\left(\frac{2\mu}{\tilde{\lambda}+2\mu}\right)\frac{1}{r^2}\int_a^r T(r,t)rdr - \frac{1}{8}\left(\frac{4\tilde{\lambda}+6\mu}{\tilde{\lambda}+2\mu}\right)r^2\omega^2 \\ &+\left(\frac{2\mu+2\tilde{\lambda}}{\tilde{\lambda}+2\mu}\right)c_1 - \left(\frac{2\mu}{\tilde{\lambda}+2\mu}\right)\frac{c_2}{r^2}\end{aligned} \tag{54}$$

$$\begin{aligned}\sigma_{\theta\theta} = &\left(\frac{2\mu}{\tilde{\lambda}+2\mu}\right)\left\{\frac{1}{r^2}\int_a^r T(r,t)rdr - T\right\} \\ &-\left(\frac{4\tilde{\lambda}+2\mu}{\tilde{\lambda}+2\mu}\right)\frac{1}{8}r^2\omega^2 + \left(\frac{2\tilde{\lambda}+2\mu}{\tilde{\lambda}+2\mu}\right)c_1 + \left(\frac{2\mu}{\tilde{\lambda}+2\mu}\right)\frac{c_2}{r^2}\end{aligned} \tag{55}$$

The unknowns $c_1(t)$ and $c_2(t)$ may be determined by applying the mechanical boundary conditions.

5 RESULTS AND DISCUSSIONS

To investigate the accuracy of the presented formulations, an example is chosen from Ref. [1], where the coupled thermeolasticity of a disk is analyzed using the finite element method. In this example, a stationary disk made of aluminum, with the Lame′ constants $\lambda = 40.4$ GPa, $\mu = 27$ GPa and $\alpha = 23 \times 10^{-6}\ \mathrm{K}^{-1}$, $\rho = 2707\ \mathrm{kg/m^3}$, $\kappa = 204\ \mathrm{W/m \cdot K}$ and $c = 903\ \mathrm{J/kg \cdot K}$ is considered. The nondimensional inner and outer radii of the disk is given as

$a = 1$ and $b = 2$, respectively. The inside boundary of the disk is assumed to be radially fixed, but exposed to a step function heat flux. The outside boundary is traction free with zero temperature change. The initial conditions for the displacement, velocity, temperature, and the rate of temperature are assumed to be zero.
In the case of zero angular velocity, assuming that $C = 0.02$ and $\hat{t}_0 = 0.64$, the time variation of the nondimensional temperature and radial displacement at mid-radius of the disk are plotted in Figs. 1. Good agreements are observed between the results of presented analytical method and those obtained using the Galerkin finite element method in Ref. [1].

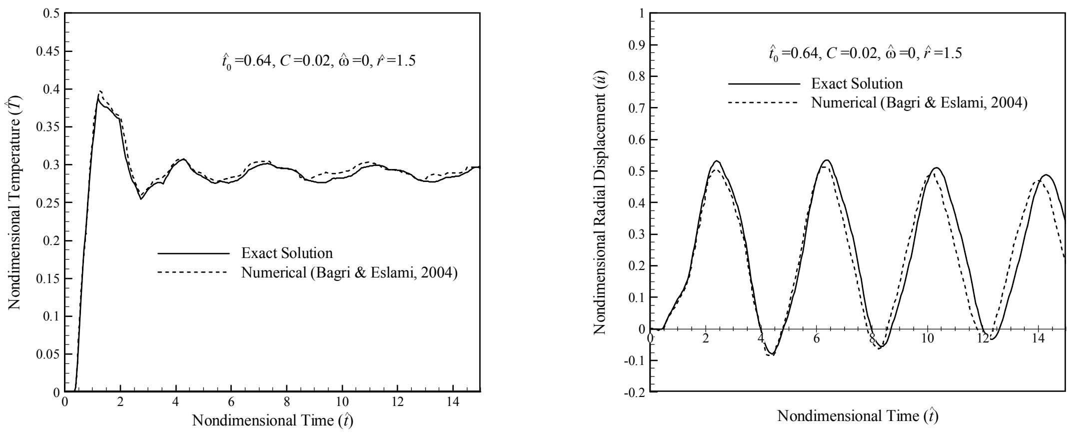

Figure 1: Time history of the nondimensional temperature and displacement at mid-radius of the stationary disk

Assuming that the disk is rotating with nondimensional angular velocity 0.01, the time histories of temperature and radial displacement at mid-radius of the disk for the different theories of thermoelasticity are shown in Fig. 2. Moreover, For these theories, the time histories of radial stress and tangential stress are plotted in Figs. 3 and 4, respectively. In this case, the reference temperature is considered to be 293 K.

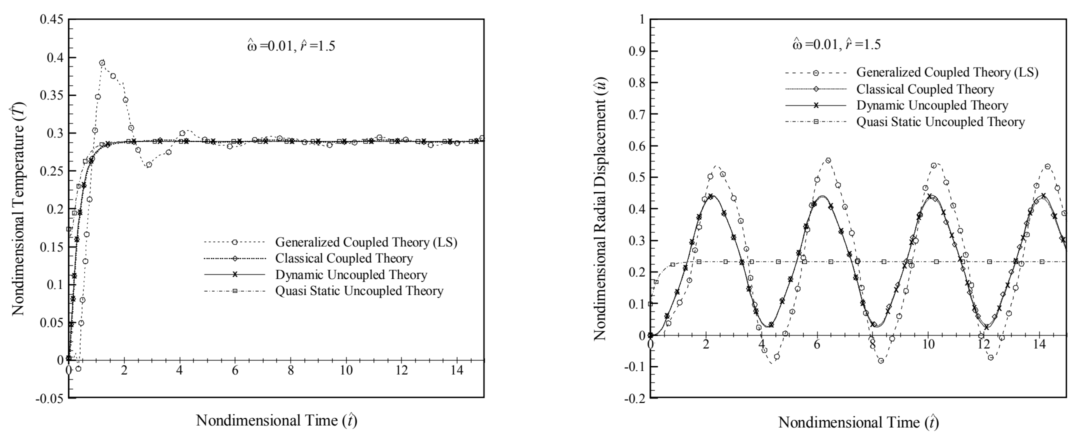

Figure 2: Time history of the nondimensional temperature and displacement at mid-radius of the rotating disk for different theories of thermoelasticity

As shown in Figs. 2-4, when thermal shock load is applied, the generalized coupled theory based on LS model leads to larger maximum value of the curves for temperature, displacement and stresses compared to other theories.
The classical coupled theory and uncpuled theories of thermoelasticity predict an infinite propagation speed for the thermal disturbances. In other words, when $\hat{t}_0 = 0$ the hyperbolic heat conduction equation (11) reduces to a parabolic equation with infinite speed for thermal wave propagation. Moreover, this Fig. 2 shows that in the case of dynamic uncoupled solution, $C = 0$, the influence of temperature field on displacement filed is ignored and thus the radial displacement varies harmonically along the time with constant amplitudes. For coupled thermoelastic solutions, the displacement amplitudes are decreasing along the time axis. The reason is that for $C \neq 0$, damping term appears in the heat conduction equation and, therefore, the energy dissipation occurs in the system.

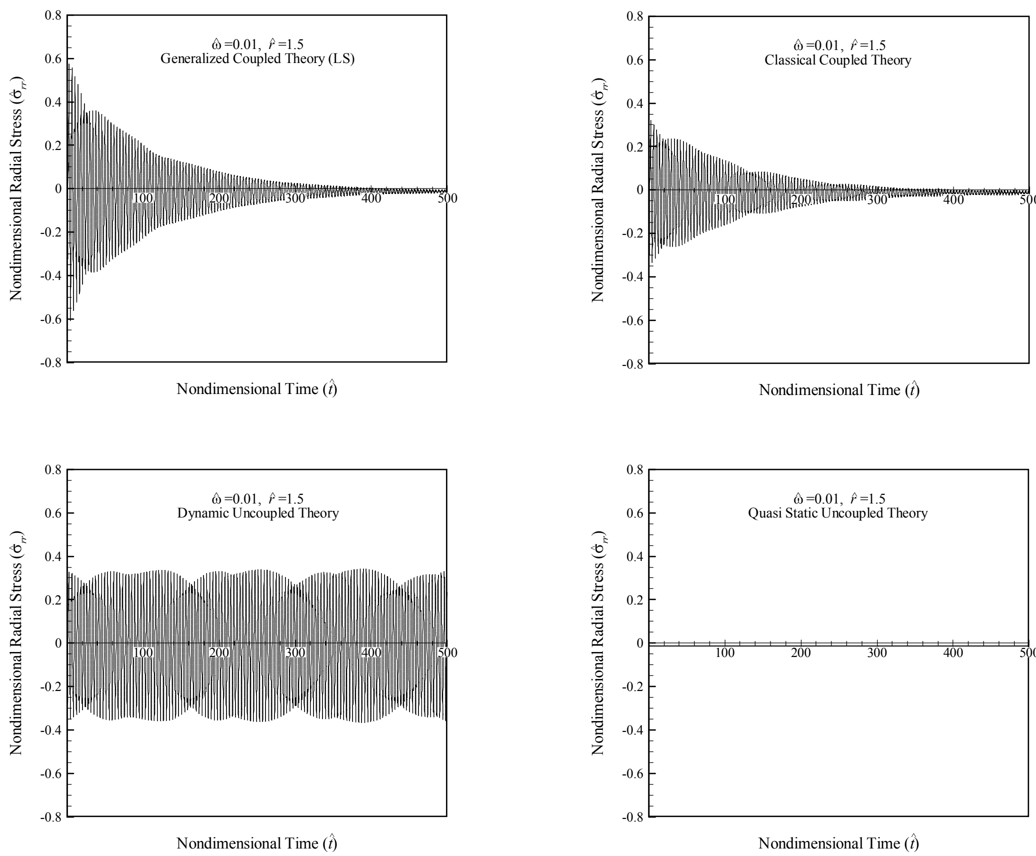

Figure 3: Time history of the nondimensional radial stress at mid-radius of the rotating disk for different theories of thermoelasticity

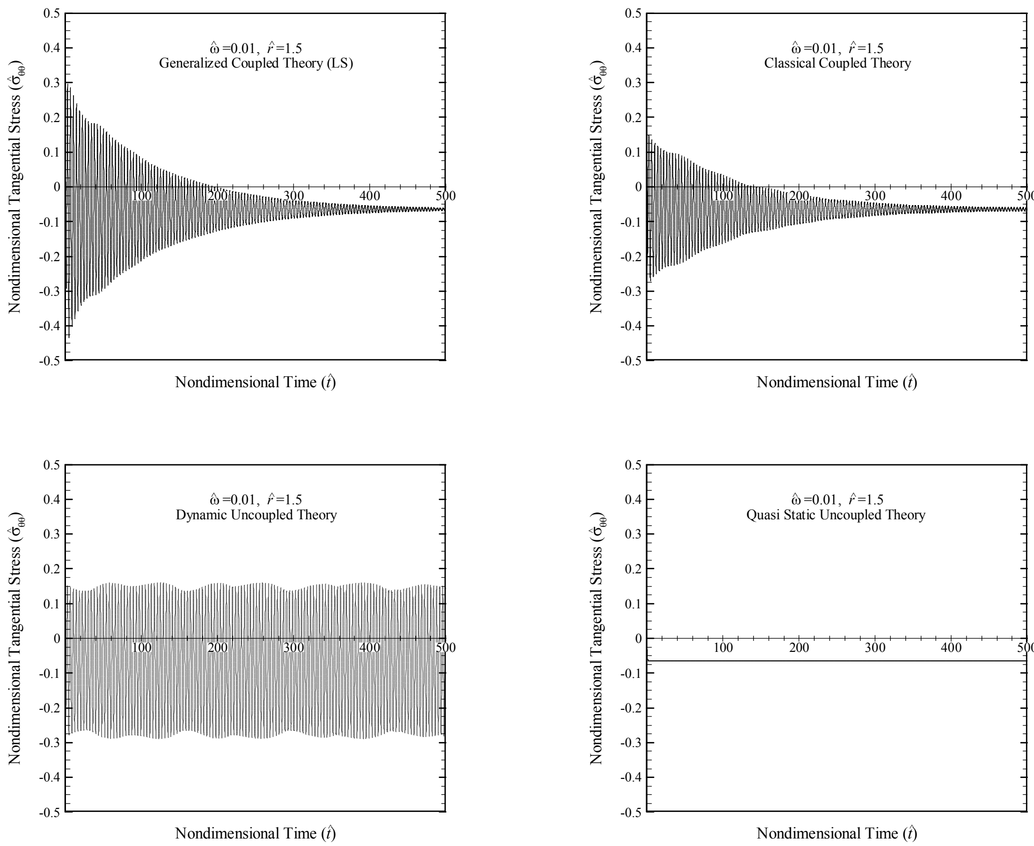

Figure 4: Time history of the nondimensional tangential stress at mid-radius of the rotating disk for different theories of thermoelasticity

The radial distribution of nondimensional temperature and stress components for different theories of thermoeleasticity at different values of the time are shown in Figs. 5.
In these figures, the temperature wave front is clearly observed from the figure related to generalized coupled solution. In this figure, times $\hat{t} = 0.25,\ 0.5$ and 0.75 show the temperature wave propagation, while times $\hat{t} = 1,\ 1.25$ indicate the wave reflection from the outer radius of the disk. However, the temperature gradient along the radius is smooth for the classical coupled and uncpuled theories of thermoelasticity due to the infinite speed of thermal wave disturbances in this theories. The elastic wave fronts are clearly seen from the figures related to coupled and dynamic uncoupled solutions, while the radial distribution of radial stress related to quasi static uncoupled solution is smooth at different values of the time.

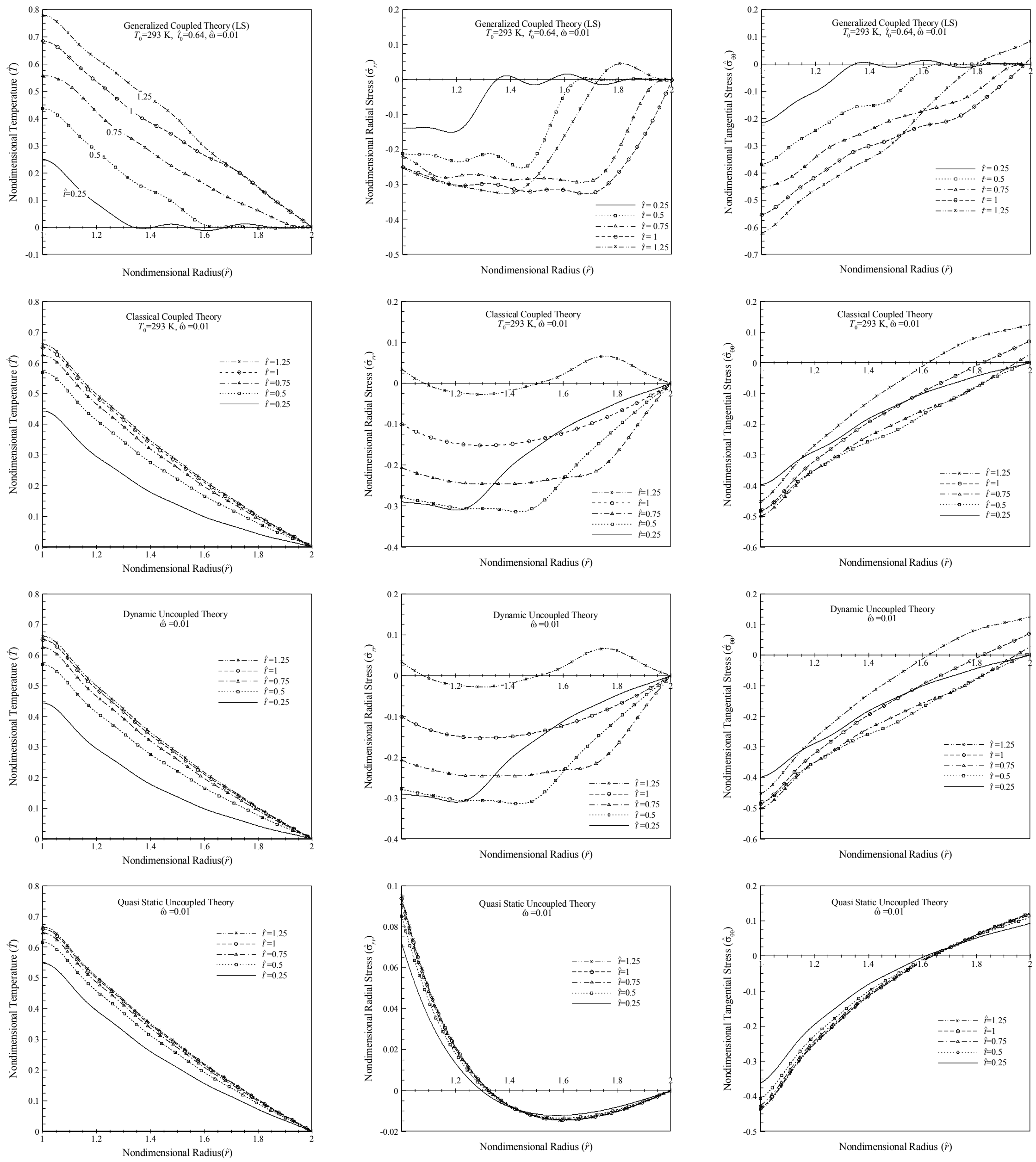

Figure 5: Radial distribution of nondimensional temperature and stress components for different theories of thermoeleasticity.

6 CONCLUSIONS

In this study, thermoelasticity problems based on the classical and generalized coupled theories, and dynamic and quasi static uncoupled theories for a rotating disk are solved using a fully analytical procedure. Assuming that the disk is subjected to an arbitrary heat transfer and traction at its inner and outer radii, closed form formulations are presented for temperature and displacement fields. The procedure used in this work, is based on the finite Hankel transform. To validate the formulations, the results of this paper are compared with those obtained using the numerical method in the literature, which show good agreement.

The radial distributions and time histories of temperature, displacement and stresses for the different theories of thermoelasticity in the disk are plotted and compared to each other. Comparison between different theories of thermoelasticity shows that under thermal shock loading, generalized coupled theory based on Lord–Shulman model predicts larger temprature and stresses compared to the other theories. Therefore, for specialized applications involving sudden temperature changes in short periods of time, the disk should be designed using some modified coupled thermoelasticity models with the finite speed of wave propagation such as Lord-Shulman (LS).

REFERENCES

[1] A. Bagri, M. Eslami, Generalized coupled thermoelasticity of disks based on the Lord–Shulman model, Journal of Thermal Stresses, 27 (2004) 691-704.

[2] M. Bakhshi, A. Bagri, M. Eslami, Coupled thermoelasticity of functionally graded disk, Mechanics of Advanced Materials and Structures, 13 (2006) 219-225.

[3] A. Bagri, M.R. Eslami, Generalized coupled thermoelasticity of functionally graded annular disk considering the Lord–Shulman theory, Composite Structures, 83 (2008) 168-179.

[4] M. Abbasi, M. Sabbaghian, M.R. Eslami, Exact closed-form solution of the dynamic coupled thermoelastic response of a functionally graded Timoshenko beam, Journal of Mechanics of Materials and Structures, 5 (2010) 79-94.

[5] A. Afshar, M. Abbasi, M. Eslami, Two-dimensional solution for coupled thermoelasticity of functionally graded beams using semi-analytical finite element method, Mechanics of Advanced Materials and Structures, 18 (2011) 327-336.

[6] M. Jabbari, H. Dehbani, M.R. Eslami, An exact solution for classic coupled thermoelasticity in spherical coordinates, ASME J. Pressure Vessel Technol., 132 (2010) 031201.

[7] M. Jabbari, H. Dehbani, M.R. Eslami, An exact solution for classic coupled thermoelasticity in cylindrical coordinates, Journal of Pressure Vessel Technology, 133 (2011) 051204.

[8] M. Jabbari, H. Dehbani, Exact solution for lord-shulman generalized coupled thermoporoelasticity in cylindrical coordinates, Encyclopedia of Thermal Stresses, (2014) 1399-1411.

[9] M. Jabbari, H. Dehbani, Exact solution for lord-shulman generalized coupled thermoporoelasticity in spherical coordinates, Encyclopedia of Thermal Stresses, (2014) 1412-1426.

[10] A.H. Akbarzadeh, M. Abbasi, M.R. Eslami, Coupled thermoelasticity of functionally graded plates based on the third-order shear deformation theory, Thin-Walled Structures, 53 (2012) 141-155.

[11] S.M. Hosseini, M.H. Abolbashari, Analytical solution for thermoelastic waves propagation analysis in thick hollow cylinder based on Green–Naghdi model of coupled thermoelasticity, Journal of Thermal Stresses, 35 (2012) 363-376.

[12] A.R. Shahani, S.M. Bashusqeh, Analytical solution of the coupled thermo-elasticity problem in a pressurized sphere, Journal of Thermal Stresses, 36 (2013) 1283-1307.

[13] M.A. Kouchakzadeh, A. Entezari, Analytical solution of classic coupled thermoelasticity problem in a rotating disk, Journal of Thermal Stresses, 38 (2015) 1269-1291.
[14] R.B. Hetnarski, M.R. Eslami, Thermal Stresses-Advanced Theory and Applications, Springer, 2009.
[15] H.W. Lord, Y. Shulman, A generalized dynamical theory of thermoelasticity, Journal of the Mechanics and Physics of Solids, 15 (1967) 299-309.
[16] J. Prevost, D. Tao, Finite element analysis of dynamic coupled thermoelasticity problems with relaxation times, Journal of applied mechanics, 50 (1983) 817-822.
[17] G. Cinelli, An extension of the finite Hankel transform and applications, International Journal of Engineering Science, 3 (1965) 539-559.